

# Modeling and Analysis of a Novel Mppt for Pmsg Based Stand-Alone Wind Energy Conversion

Ballagiri Suresh & P.Harikrishna

M.Tech Scholar Sai Tirumala NVR Engineering College, India  
Asst.Professor Sai Tirumala NVR Engineering College India

## ABSTRACT

*This thesis presents a novel control strategy for the operation of a direct-driven permanent-magnet synchronous generator-based stand-alone variable-speed wind turbine. The battery charger employs a boost converter cascaded with a Greatz bridge that can harvest the maximum power from wind turbine. Also, a buck converter is connected in series with the boost stage to ensure a constant voltage. This system can extract maximum power over the entire wind speed range and the battery charging can be realized through conventional techniques. Simulation results are presented to depict the existence of maximum power points in wind generator.*

## INTRADUCTION

Continuing development of modern society is contingent on the sustainability of energy. The vulnerability of the current energy chain, reliant on non renewable fossil fuel resources, will provoke a collapse in our society with the exhaustion of its natural reserves [1]. That is why wind power energy is strongly advocated in projects and studies where the following factors are considered:

- High cost of hydro- and thermo electrical generation
- Areas with fairly high average wind speeds (>3 m/s)

- Need to feed remote loads, where a transmission network is uneconomical
- Nonexistence of rivers or other energetic hydro resources in close proximity
- Need for renewable, non-polluting energy

Wind power energy is derived from solar energy, due to uneven distribution of temperatures in different areas of the Earth. The resulting movement of air mass is the source of mechanical energy that drives wind turbines and the respective generators. Across Europe there are several leading wind energy markets: Germany, Spain, Denmark, Great Britain, Sweden, the Netherlands, Greece, Italy, and France.

There are several European companies exporting products and technology. U.S. wind resources are also appreciable. U.S. wind resources are large enough to generate more than 4.4 trillion kWh of electricity annually. There are sufficient wind intensities for power generation on mountainous areas and deserts, as well as in the midlands, spanning the wind belt in the Great Plains states. North Dakota alone is theoretically capable (if there were enough

transmission capacity) of producing enough wind-generated power to meet more than one-third of U.S. demand. According to the Battelle Pacific Northwest Laboratory, wind energy can supply about 20 % of US. electricity, with California having the largest installed capacity. In South America, Brazil has vast wind potential because of its extended Atlantic shore. Particularly in the Brazilian northeast states, there are scarce hydroelectric resources. However, the integrated generation of wind and solar power is a powerful alternative. The Brazilian wind power potential is evaluated at 63 trillion kWh/yr. **2.2**

### APPROPRIATE LOCATION

To select the ideal site for placement of wind power turbines, it is necessary to study and observe the existence of enough wind to make extraction of energy possible at a desired rate. Although flat plains may have steady strong winds, for small-scale wind power the best choice is usually along dividing lines of waters (i.e., the crests of mountains and hills). In those geographical locations, there is good wind flow perpendicular to the crest direction. Some basic characteristics to be observed for defining a site are:

- Wind intensities in the area
- Distance of transmission and distribution networks

- Topography
- Purpose of the energy generated
- Means of access

### 2.3 EVALUATION OF WIND INTENSITY

The energy captured by the rotor of a wind turbine is proportional to the cubic power of the wind speed. Therefore, it is very important to evaluate the historical wind power intensity ( $W/m^2$ ) to access the economical feasibility of a site, taking in account seasonal as well as year-to-year variations in the local climate. To estimate the wind power mechanical capacity,  $P$ , Bernoulli's equation is used with respect to the mass flow derivative of its kinetic energy,  $K_e$ .

$$P = \frac{dK_e}{dt} = \frac{1}{2} v^2 \frac{dm}{dt} \quad \text{-- (2.1)}$$

The mass flow rate per second is given by the derivative of the quantity of mass,  $dm/dt$ , of the moving air that is passing with velocity  $v$  through the circular area  $A$  swept by the rotor blades as suggested in figure 2.1. According to equation for any average flow ( $\bar{Q} = A\bar{v}$ ) of a fluid, the upstream flow of mass can be given in terms of the volume of air  $V$  as

$$\frac{dm}{dt} = \rho \frac{dv}{dt} = \rho A \bar{v} \quad \text{-- (2.2)}$$

where  $\rho = m/V$  is the air density in  $kg/m^3$  ( $=1.2929 \text{ kg/m}^3$  at  $0^\circ C$  and at sea level) and  $A$  is the surface swept by the rotor or blades ( $m^2$ ).

The effective power extracted from wind is derived from the airflow speed just reaching the

turbine,  $v_1$ , and the velocity just leaving it,  $v_2$ . The number of blades must also be considered. Equation (2.2) considers the average speed  $(v_1 + v_2)/2$  passing through area  $A$  of the rotor blades (i.e., effectively acting on the rotor blades). Therefore, equation (2) becomes

$$\frac{dm}{dt} = \frac{\rho A (v_1 + v_2)}{2} \quad \text{-- (2.3)}$$

Also, there is a difference in the kinetic energy (usually expressed in  $\text{kg.m/s} = 9.81 \text{ W}$ ) in the wind speed just reaching and just leaving the turbine. A

net wind mechanical power of the turbine is imposed by this kinetic energy difference, which may be estimated by equation (2.1) as

$$P_m = \frac{dK_e}{dt} = \frac{1}{2} (v_1^2 - v_2^2) \frac{dm}{dt} \text{ W/m}^2 \quad \text{-- (2.4)}$$

Combining equations (2.3) and (2.4), the following power is calculated:

$$P_m = \frac{dK_e}{dt} = \frac{1}{4} \rho A (v_1^2 - v_2^2) (v_1 + v_2) \quad \text{-- (2.5)}$$

Whose upstream wind speed,  $v_1$  is used to give

$$P_m = \frac{1}{4} \rho A v_1^3 \left(1 - \frac{v_2^2}{v_1^2}\right) \left(1 + \frac{v_2}{v_1}\right) \quad \text{-- (2.6)}$$

Or

$$P_m = \frac{1}{2} \rho C_p A v_1^3 \quad \text{-- (2.7)}$$

$$\text{Where } C_p = \left(1 - \frac{v_2^2}{v_1^2}\right) \left(1 + \frac{v_2}{v_1}\right) / 2$$

is the power coefficient or rotor efficiency as expressed by Betz.

If  $C_p$  is considered a function of  $v_2/v_1$ , the maximum of such a function can be obtained for  $v_2/v_1 = \frac{1}{3}$  as  $C_p = \frac{16}{27} = 0.5926$ .

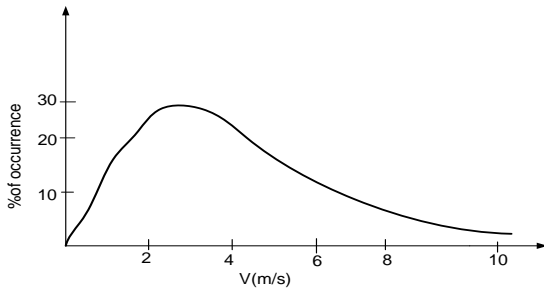
This value is known as the Betz limit, the point at which if the blades were 100% efficient, the wind turbine would no longer work because the air (having given up all its energy) would stop entirely after passing its blades. In practice, the collection efficiency of a rotor is not as high as 59%; a more typical efficiency is between 35 and 45%. To achieve the best designs, several sources of data,

such as meteorological maps, statistical functions, and visualization aids, should be used to support the analysis of the wind potential.

#### (a) METEOROLOGICAL MAPPING

There are meteorological maps showing curves connecting the same intensity of average wind speed. Although such maps may yield valuable information, they are not sufficient for a complete analysis because the meteorological data acquisition stations do not look only for a determination of the wind potential for power energy use. Therefore, a final decision on the site will be made only after a convenient local

selection procedure and thorough data acquisition. Local wind power is directly proportional to the distribution of speed, so that different places that have the same annual average speed can present very distinct values of wind power. Figure 2.2 displays a typical wind speed distribution curve for a given site. That distribution can be made monthly or annually. It is determined through bars of occurrence numbers, or percentile of occurrence, for each range of wind speed over a long period of time. It is usually observed as a variation of wind linked with climate changes in the area. It is typical in temperate climates to have summer characterized as a season of little wind and winter as a season of stronger winds.



When the wind speed is lower than 3 m/s (referred to as a calm period), the power becomes very limited for the extraction of energy and the system should be stopped. Therefore, for power plants, calm periods will determine the time required for energy storage. As discussed next, power distribution varies according to the intensity of the wind and with

the power coefficient of the turbine. A typical distribution curve of power assumes the form shown in Figure 2.3. Sites with high average wind speeds do not have calm periods, and there is not much need of storage. However, high wind speed may cause structural problems in a system or in a turbine.

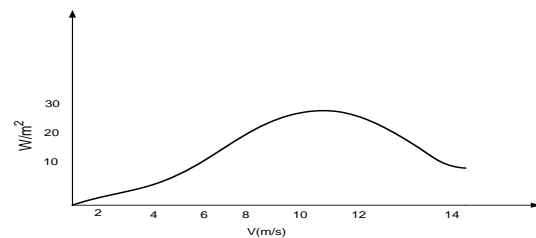


Figure 2.3 Power distribution.

#### ANALYSIS OF WIND SPEED BY VISUALIZATION

If a site being evaluated is not close to meteorological stations, a good practical suggestion is to observe the existing trees. Their deformation level will serve as a good indicator of the wind speeds in the area. The intensity of the wind increases with height; therefore, trees of larger span are reached by more intense winds, which can harm their growth. The following levels of tree deformation are recognized:

- Brush. When branches are on the lee side (the side exposed to wind), especially in the absence of leaves the winds are weak.
- Flag. Branches are the lee barriers (the static trunks in their original position, free to windward), in other words, the side from which the wind blows.
- Lie down. The wind is strong enough to produce permanent deformations in trunks and branches.

•Shear. The wind is always strong, to the point of breaking branches, giving the impression that they were cut uniformly.

•Rug of trees. The wind energy is so strong that it limits the growth of trees to some inches of the soil, giving the impression that the trees form a rug.

For small wind power installations, a visual assessment of the wind intensity is described in Table 2.1, which is an adaptation of the Beaufort table. The International Committee of Meteorology adopted such a table in 1874; wind measurement using anemometers did not begin until 1939.

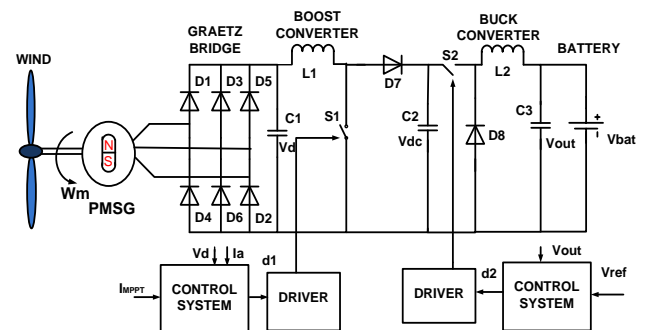
#### 2.4. TOPOGRAPHY

The analysis of topography is very important when choosing a site. This is an important point when mountainous locations are under consideration. For those areas, the wind speed increases on the front side of the mountain and decreases on the opposite side. In plane areas, the position of tree barriers should be observed with respect to the wind, as their proximity to the place chosen for turbine installation is critical. There should be a maximum of free space between tree barriers and the power plant, to avoid any slowing down of the wind. With increased altitude, the movement of a wind draft takes a more complex form, due to different land shapes. Thus, it is necessary to have a reasonable knowledge of the characteristics of the soil to be occupied. The roughness of the ground surface causes wind shear, which changes significantly with altitude. Some data collected at Merida Airport in Mexico show that the

wind speed can be four to five times higher at an altitude of about 450m with respect to the ground surface, and then it starts to decrease again. At about 100m from the surface, many places on Earth have a wind speed sufficient for wind energy, but the costs of such high installation severely limit a decision in favour of using such heights.

#### DESIGN OF PROPOSED CONVERTER

The proposed charger feasible to small wind energy conversion systems shown in the fig.4.1. The wind turbine is connected to an axial flux PMSG which is rated at 6KW for the generated power, 10 poles & electrical frequency of 60HZ. The battery bank is composed by two lead-acid batteries, both rated at 12V/150Ah.



#### DYNAMIC MODEL OF THE PMSG:

Synchronous machine models for power system analysis are usually based on the assumption that the magnetic flux distribution in the rotor is sinusoidal. With this assumption the flux can entirely be described by a vector and thus the internal voltage E induced in the stator by the permanent magnets can be expressed as follows:

$$E = j \cdot \omega_{gen} \psi_{PM} = j \cdot 2\pi f \cdot \psi_{PM} \quad \text{-- (4.1)}$$

where  $\omega_{gen}$  is the electrical generator rotational speed,  $\psi_{PM}$  is the flux provided by the permanent magnets of the rotor, and  $f$  is the electrical frequency. The excitation voltage  $E$  is proportional with the electrical speed of the generator. The equations of a PMSG can be expressed directly from the equations of a DC excited SG, with the simplification that a PMSG does not have damper windings. The voltage equations of the generator, expressed in the rotor-oriented dq-reference frame RRF (the reference frame d-axis is aligned with the vector of the permanent magnet flux), can be expressed as follows:

$$U_{sd} = R_s i_{sd} - \omega_{gen} \psi_{sq} + \psi_{sd} \quad -- \quad (4.2)$$

$$U_{sq} = R_s i_{sq} + \omega_{gen} \psi_{sq} + \psi_{sd} \quad \text{in ( RRF )} \quad -- \quad (4.3)$$

with the stator flux components:

$$U_{sd} = L_d i_{sd} + \psi_{PM} \quad -- \quad (4.4)$$

$$U_{sq} = L_q i_{sq} \quad \text{in ( RRF )} \quad -- \quad (4.5)$$

where  $U_{sd}$  and  $U_{sq}$  are the terminal stator voltage components,  $i_{sd}$  and  $i_{sq}$  are the stator current components,  $L_d$  and  $L_q$  are the stator inductances in the dq-reference frame. As in stability studies the stator transients can typically be neglected, the stator voltage equations can be simplified as follows:

$$U_{sd} = R_s i_{sd} - \omega_{gen} \psi_{sq} \quad -- \quad (4.6)$$

$$U_{sq} = R_s i_{sq} + \omega_{gen} \psi_{sd} \quad \text{in ( RRF )} \quad --$$

(4.7) The electrical torque of the generator can be expressed as :

$$T_e = \frac{3}{2} * \rho * [ \psi_{sd} i_{sq} - \psi_{sq} i_{sd} ] \quad \text{in( RRF )} \quad -- \quad (4.8)$$

Expressing further the stator flux components, the electrical torque can be calculated by:

$$T_e = \frac{3}{2} * \rho * [(L_d - L_q) i_{sd} i_{sq} + \psi_{PM} i_{sq}] \quad \text{in ( RRF )} \quad --$$

(4.9) If the PMSG is assumed to be a round-rotor machine where  $L_d=L_q$ , which is a reasonable approximation for this type of generator, the electrical torque of the generator results only from the permanent magnet flux and the q-component of the stator current:

$$T_e = \frac{3}{2} * \rho * \psi_{PM} i_{sq} \quad \text{in ( RRF )} \quad -- \quad (4.10)$$

The active and reactive power of the synchronous generator are:

$$P_{gen} = \frac{3}{2} [U_{sd} i_{sd} + \psi_{sq} i_{sq}] \quad -- \quad (4.11)$$

$$Q_{gen} = \frac{3}{2} [U_{sq} i_{sd} - \psi_{sd} i_{sq}] \quad -- \quad (4.12)$$

As neither a damper nor field winding exists in a PMSG, no transient or subtransient reactances, as known for wound rotor SGs, can be defined for the PMSG.

$$x_d = x'_d = x''_d \quad -- \quad (4.13)$$

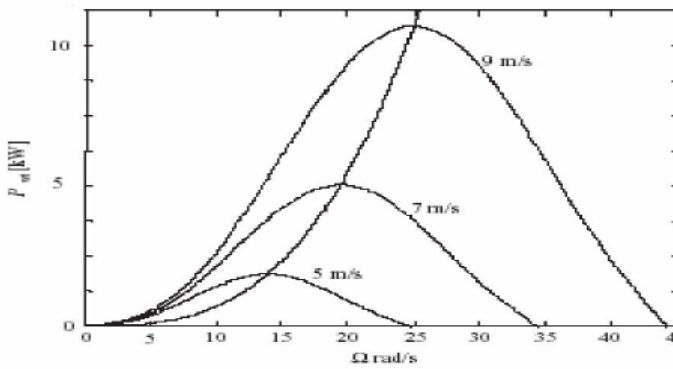
$x_d \sim$  Synchronous reactance

$x'_d \sim$  Transient reactance

$x''_d \sim$  Subtransient reactance

However, as the multi pole PMSG is a low speed application with slow dynamics, a damper winding is less important. One of the important features of the PM synchronous generator is that its output voltage is proportional to the rotor speed. Basically, as the wind speed increases, the output

power of the wind turbine increases, too. For each wind speed, there exists a MPP. The dash line shown in Fig. 4.2 represents the MPP curve of the wind turbine under different wind speed. Theoretically, under a constant power conversion coefficient  $C_p$ , the MPP curve is found to be a cubic function of the turbine speed.



## SIMULATION RESULTS

### 5.1. SIMULINK MODEL OF WIND TURBINE

In this section, simulation circuits and results are presented. The simulation circuit diagram for a wind turbine modeled in Simulink is given below:

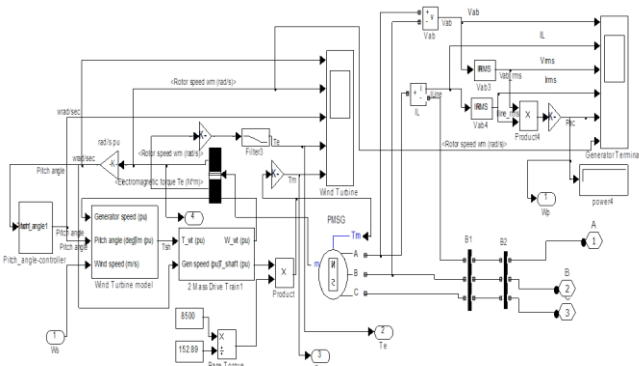


Fig .5.1 Model of Wind turbine

The control technique used in this topology for achieving MPPT is Optimal Torque Control (OTC). It is modeled in Simulink as follows:

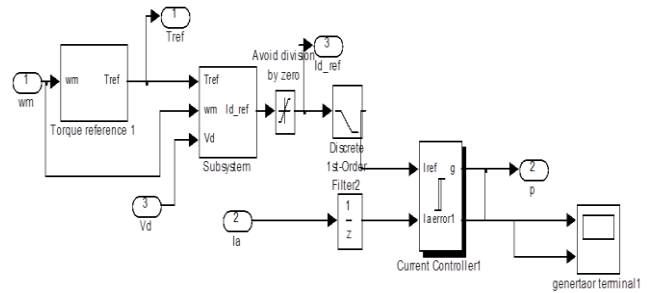


Fig. 5.2 Model achieving MPPT

The simulink model of PWM modulator is shown below

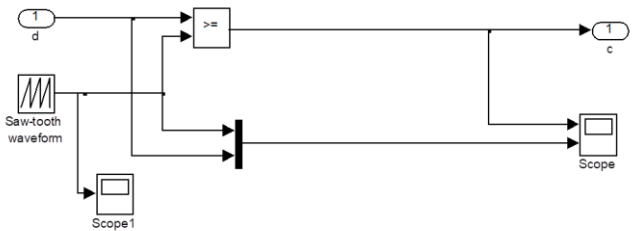


Fig. 5.3. PWM Block

### SIMULINK MODEL OF PROPOSED CONVERTER

The Simulink model of the power converters finally feeding batteries is shown below:

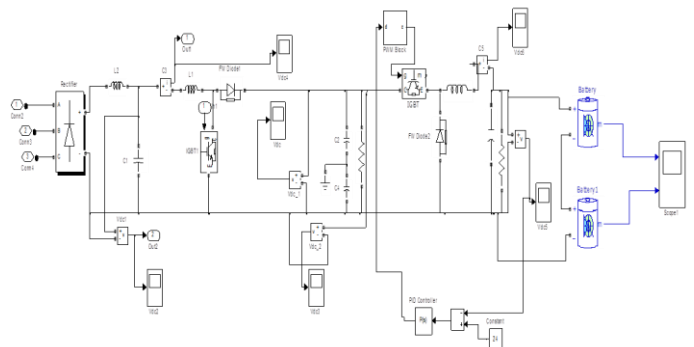


Fig.5.4. Boost and buck cascaded stage

Many control strategies can be used to get the desired voltage at buck level to feed the batteries. The control techniques used for buck converter in this topology are voltage control and sliding mode control. The ripples in the voltage controlled mode can be reduced by using the sliding mode current control also the performance achieved is satisfactory.

### SIMULATION RESULTS

The rotor speed and the mechanical torque produced by the wind turbine are shown in the fig.5.6 and fig.5.7.

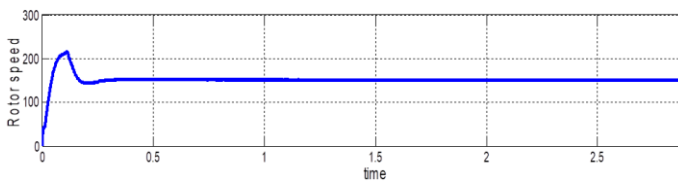


Fig. 5.5. Rotor speed of the wind turbine

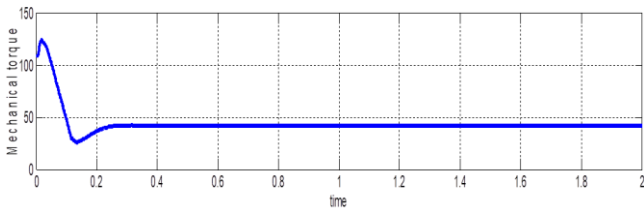


Fig. 5.6. Mechanical Torque of the wind turbine

The wind turbine is connected to the shaft which is further connected directly to PMSG as it is direct driven machine which needs no gear-box transmission system.

The electromagnetic torque generated by the Synchronous machine is shown in the fig.5.8.

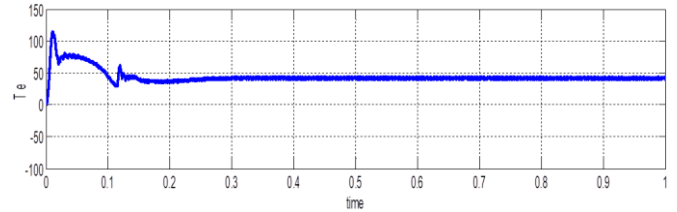


Fig.5.7. Electromagnetic torque.

The following figures gives the line values of voltage and current of the PMSG.

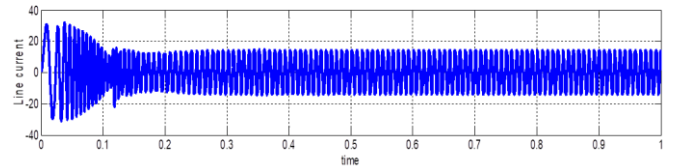
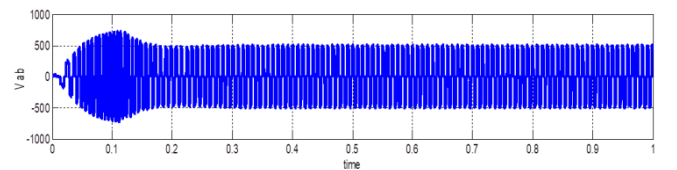
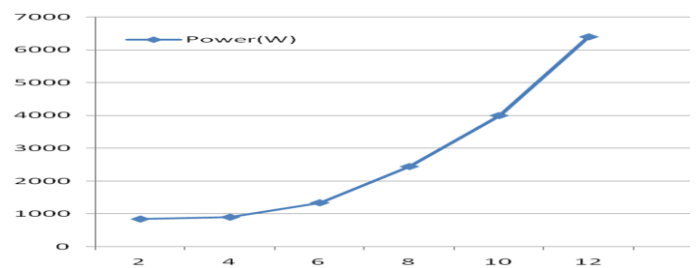
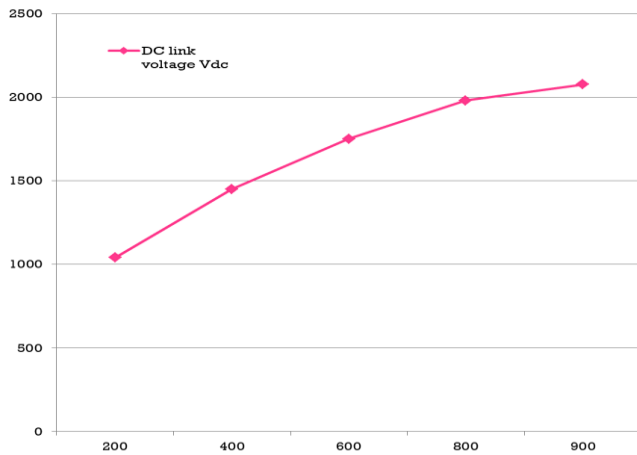


Fig.5.10. Line current obtained from the PMSG.

The following graph gives the Maximum Power Point operation for variable wind speeds. For a definite wind speed there will be a certain point where maximum power is extracted from the wind turbine. The points are plotted and MPP curve is drawn.







## CONCLUSION

The modeling of a variable speed wind turbine with a permanent magnet synchronous generator has been developed and implemented in MATLAB/Simulink. This project has presented a three stage power converter as a battery charger feasible to small wind energy systems. The developed prototype is more efficient to transfer the maximum power from the wind turbine to the battery bank over the entire wind speed range and also in case where it is necessary to vary the number of connected batteries. In this project, maximum power point tracking concept has been presented in terms of the adoption of the generator speed according to instantaneous wind speed control strategies.

The control technique used for the buck converter is closed loop voltage control method and the MPPT used is Optimal Torque Control method.

## REFERENCES

[1]. J. Smith, R. Thresher, R. Zavadil, E. DeMeo, R. Piwko, B. Ernst, and T. Ackermann, "A mighty wind," *IEEE Power Energy Mag.*, vol. 7, no. 2, pp. 41–51, Mar./Apr. 2009

[2]. B. S. Borowy and Z. M. Salameh, "Dynamic response of a stand-alone wind energy conversion system with battery energy storage to a wind gust," *IEEE Trans. Energy Convers.*, vol. 12, no. 1, pp. 73–78, Mar. 1997.

[3]. Z. Chen and E. Spooner, "Grid interface options for variable-speed, permanent-magnet generators," *IEE Proc. Electr. Power Appl.*, vol. 145, no. 4, pp. 273–283, Jul. 1998.

[4]. I. R. Machado, H. M. Oliveira Filho, L. H. S. C. Barreto, and D. S. Oliveira Jr., "Wind Generation System for Charging Batteries", *Brazilian Power Electronics Conference – COBEP*, pp 371-376, 2007.

[5]. E. Koutroulis and K. Kalaitzakis, "Design of a Maximum Power Tracking System for Wind-Energy-Conversion Applications", *IEEE Transactions on Industrial Electronics*, vol. 53, no. 2, pp 486-494, April 2006.

[6]. K. Y. Lo, Y. M. Chen, Y. R. Chang, "MPPT Battery Charger for Stand- Alone Wind Power System", *IEEE Transactions on Power Electronics*, vol. 26, no. 6, pp 1631-1638, June 2011.

[7]. R. P. T. Bascopé, H. M. Oliveira Filho, L. D. S. Bezerra, C. M. T. Cruz, F. K. A. Lima, and D. S. Oliveira Jr., "Electronic Circuit for Stand- Alone Wind Energy Conversion System", *Brazilian Power Electronics Conference – COBEP*, pp 964-971, 2011.

[8]. S. M. R. Kazmi, H. Goto, H. J. Guo, O. Ichinokura, "A Novel Algorithm for Fast and Efficient Speed-Sensorless Maximum Power Point Tracking in Wind Energy Conversion Systems", *IEEE Transactions on Industrial Electronics*, vol. 58, no. 1, pp 29-36, January 2011.

[9]. A. Mirecki, X. Roboam, F. Richardeau, “Architecture Complexity and Energy Efficiency of Small Wind Turbines”, IEEE Transactions on

Industrial Electronics, vol. 54, no. 1, pp 660-670, February 2007.

[10]. G. Gamboa, C. Hamilton, J. Baker, M. Pepper, I. Batarseh, “A Unity Power Factor, Maximum Power Point Tracking Battery Charger for Low Power Wind Turbines”, Applied Power Electronics Conference and Exposition – APEC, pp 143-148, 2010.

[11]. L. Maharjan, S. Inoue, H. Akagi, and J. Asakura, “State-of-charge (SOC)- balancing control of a battery energy storage system based on a cascade PWM converter,” IEEE Trans. Power Electron., vol. 24, no. 6, pp. 1628– 1636, Jun 2009.

[12]. S.Grabic, N. Celanovic, and V.A.Katic, “Permanent magnet synchronous generator cascade for wind turbine application,” IEEE Trans. Power Electron., vol. 23, no. 3, pp. 1136–1142, May 2008.

[13]. K. K. Tse, Shu-Hung Chung, and S. Y. (Ron) Hui, “Quadratic State-Space Modelling Technique for Analysis and Simulation of Power Electronic Converters” IEEE transactions on power electronics, vol. 14, No. 6, November 1999, pp 1086-

[14]. Brad Bryant, Marian K. Kazimierczuk Member “Modeling the Closed-Current Loop of PWM Boost DC–DC Converters Operating in CCM With Peak Current-Mode Control” in IEEE transactions on circuits and systems, vol. 52, no. 11, November 2005

[15]. A. Kulka, “Pitch and Torque Control of Variable Speed Wind Turbines”, M. S. thesis, Chalmers University of Technology, Goteborg, Sweden 2004.